OFDM Chirp Waveform Diversity Design With Correlation Interference Suppression for MIMO Radar

Hui Li, Yongbo Zhao, Zengfei Cheng, and Dazheng Feng

***Abstract*— The orthogonal frequency-division multiplexing (OFDM) chirp waveform has attracted much attention due to its high range resolution, low peak-to-average ratio, and large time–bandwidth product. In its application to multiple-input multiple-output radar, the correlation property of multiple OFDM chirp waveforms should be considered primarily for good detection performance. The simulation results show that high sidelobes exist in correlation functions of the conventional waveforms. In this letter, the reason for high correlation sidelobes is explored first, which is the equal subchirp durations and the same subcarrier bandwidth. Second, two new OFDM chirp waveform diversity design schemes are proposed to suppress the correlation interference. Via designing the various subchirp durations or subcarrier bandwidths specially, the high sidelobes are depressed and the correlation property is improved. Both simulation results and comparisons verify the effectiveness of the proposed methods.**

***Index Terms*— Correlation interference, multiple-input multiple-output (MIMO) radar, orthogonal frequency-division multiplexing (OFDM) chirp waveform, waveform diversity.**

I. Introduction

MULTIPLE-input multiple-output (MIMO) radar has gained much attention for its superiorities in detection performance and spatial resolution [1]–[3]. To obtain the merits mentioned above, the orthogonality of transmitted waveforms is necessary [4], [5]. What is more, in order to satisfy the application requirements, the waveforms are required to have some extra properties, e.g., the large time–bandwidth product, low peak-to-average ratio, and no range-Doppler coupling. Since the OFDM chirp waveform can fulfill some of the requirements gracefully, it becomes a popular choice for MIMO radar recently.

An OFDM signal was first presented in the radar system for higher bandwidth to improve range resolution [6], and then OFDM became a hot research topic, which concerns the ambiguity function [7], moving target detection performance [8], and so on. A major problem of the OFDM signal is the fast variation of the signal envelope, and some optimizations were implemented to reduce the peak-to-average power ratio (PAPR) [9], [10]. As the chirp signal has some superiorities such as high range resolution, good Doppler tolerance, and constant modulus, it has great potential in radar application. Hence, the OFDM principle was combined with the chirp waveform to resolve the problem of high PAPR and improve the Doppler tolerance property. When OFDM chirp waveform is applied to MIMO radar, multiple OFDM chirp signals should be generated based on a chirp basis. Thus, a novel OFDM chirp waveform design scheme consisting of the modulation and demodulation algorithm was proposed for multiple transmitters in MIMO radar [11], [12], but the correlation property or ambiguity function was not considered adequately, and the orthogonal waveforms are generated at the cost of chirp repetition. Reference [13] analyzed the challenges in implementing the OFDM chirp waveforms on practical systems and proposed a novel signal processing algorithm to solve the problem. In [14], an effective design scheme was presented for application potential, which includes OFDM chirp basis design and random matrix modulation. The designed waveforms have the superiorities of constant time domain and almost constant frequency-domain modulus, large time–bandwidth product, and low peak-to-average ratio. But there are some high correlation sidelobes that may lead to false detection. Considering the improvement of target detection performance, the correlation interference should be further suppressed.

In this letter, the reason for the high correlation sidelobes of the conventional OFDM chirp waveforms is explored, and two new OFDM chirp waveform diversity design schemes are proposed accordingly to suppress the correlation interference. The subchirp durations or subcarrier bandwidths are assumed various and designed specially to depress the high sidelobes of correlation functions. The remaining sections are organized as follows. Section II introduces the signal model and correlation function of the OFDM chirp diverse waveform, resulting in the causation of the high correlation sidelobes. The new waveform design methods for correlation interference suppression are illustrated in Section III. The design examples and simulation results are provided in Section IV. Finally, Section V concludes this letter.

II. Signal Model of OFDM Chirp Diverse Waveform

Based on the chirp waveform, the OFDM chirp waveform was proposed, which contains multiple chirp signals of different carrier frequencies or temporal durations. For MIMO radar, multiple OFDM chirp waveforms should be designed

Manuscript received December 25, 2016; revised March 7, 2017; accepted April 6, 2017. Date of publication May 2, 2017; date of current version June 22, 2017. *(Corresponding author: Hui Li.)*

H. Li, Y. Zhao, and Z. Cheng are with Xidian University, National Laboratory of Radar Signal Processing, Xian 710071, China (e-mail: lihui1990happy@126.com).

D. Feng is with Xidian University, School of Electronic Engineering, Xian 710071, China.

Color versions of one or more of the figures in this letter are available online at http://ieeexplore.ieee.org.

Digital Object Identifier 10.1109/LGRS.2017.2693681

1545-598X © 2017 IEEE. Personal use is permitted, but republication/redistribution requires IEEE permission.
See http://www.ieee.org/publications_standards/publications/rights/index.html for more information.

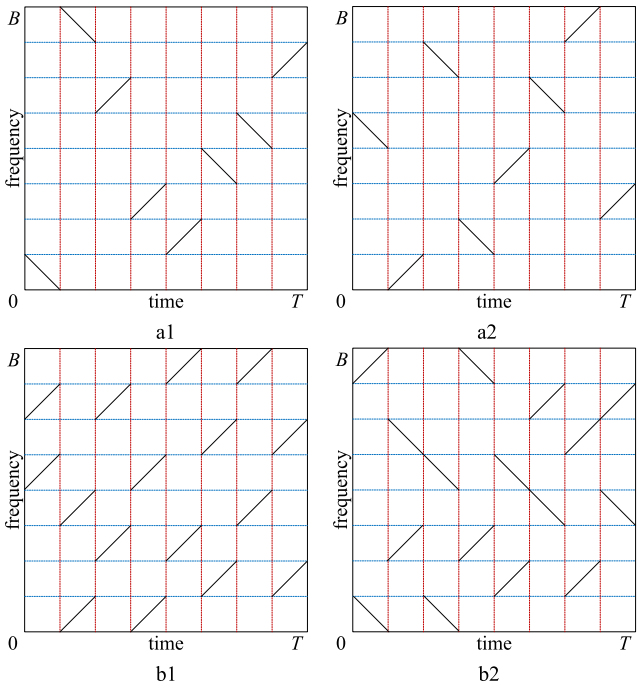

Fig. 1. Implementations of conventional OFDM chirp waveforms.

for multiple transmit antennas. Thus, a chirp basis should be designed first, and then different waveforms are constructed by diverse occupied subchirps. From a practical point of view, the subchirp signals should have equal or reverse chirp rates for reducing the hardware complexity [14]. Based on such a chirp basis, the OFDM chirp waveforms with M temporal chirps and N subcarriers can be expressed as

$$s_p(t) = \sum_{m=0}^{M-1}\sum_{n=0}^{N-1} u(t-mT_b) \cdot \exp[j2\pi(f_{mn}(t-mT_b)+k_{mn}(t-mT_b)^2/2)] \quad (1)$$

where $s_p(t), p = 1, 2, \ldots, P$ is the transmit signal of the pth antenna, P denotes the number of transmit antennas, and $t, 0 \le t \le T$, represents the time samples of the signal. $u(t) = 1, 0 \le t \le T_b$ is the rectangular windowing function, T_b is the subchirp duration and $T = MT_b$ is the pulse duration of the waveform. B_b represents the subcarrier bandwidth and $B = NB_b$ denotes the available bandwidth of the signal. f_{mn} and k_{mn} denote the starting frequency and chirp rate of the nth subcarrier at mth subchirp duration of signal $s_p(t)$, respectively. $f_{mn} = nB_b$ and $k_{mn} = B_b/T_b$ if an upchirp basis signal is used, whereas $f_{mn} = (n+1)B_b$ and $k_{mn} = -B_b/T_b$ for the downchirp basis signal.

According to the signal model in (1), conventional OFDM chirp waveforms of eight subcarriers and eight subchirp durations with a hybrid chirp basis are designed [14]. Their implementations are shown in Fig. 1. The available bandwidth is $B = 400$ MHz, and the pulse duration is $T = 8$ μs. a1 and a2 are waveforms with one subcarrier occupied in each subchirp duration, whereas two subchirp basis signals are used simultaneously at each subchirp in waveforms b1 and b2.

The conventional waveforms in Fig. 1 have the superiorities of high range resolution, large time–bandwidth product, no range-Doppler coupling, and so on. However, the transmit

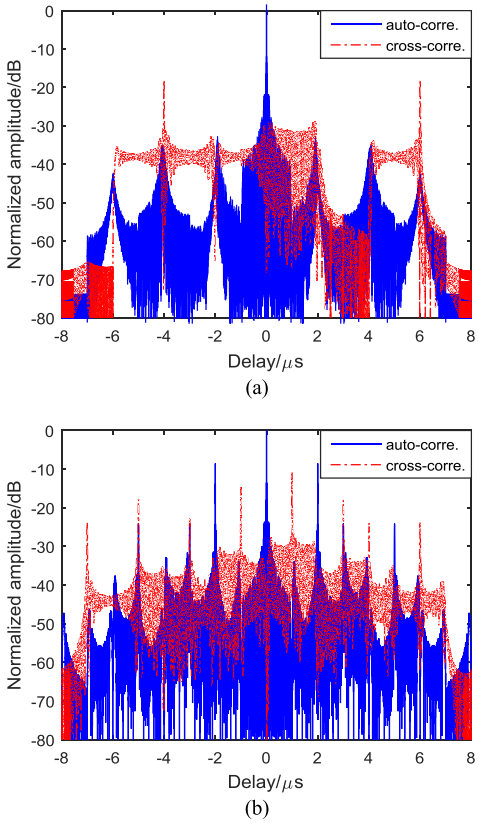

Fig. 2. Correlation functions of conventional OFDM chirp waveforms. (a) Correlation function of a1 and a2. (b) Correlation function of b1 and b2.

signals of MIMO radar should have low cross-correlation levels and autocorrelation sidelobe levels for the separation on receive. Thus, it is necessary to analyze the correlation functions of the OFDM chirp waveforms. The correlation function between the pth waveform and the qth waveform is defined as

$$c_{pq}(\tau) = \begin{cases} \int_{\tau}^{T} s_p(t)s_q^*(t-\tau)dt, & 0 \le \tau < T \\ \int_{0}^{T+\tau} s_p(t)s_q^*(t-\tau)dt, & -T < \tau < 0 \end{cases} \quad (2)$$

where τ is the time delay. $c_{pq}(\tau)$ is the cross-correlation function if $p \ne q$, whereas $c_{pp}(\tau)$ represents the autocorrelation function while $p = q$. The autocorrelation functions and the cross-correlation functions of the waveforms in Fig. 1 are calculated by (2) and plotted in Fig. 2. The autocorrelation function of a1 and the cross-correlation function between a1 and a2 are shown in Fig. 2(a). Fig. 2(b) plots the autocorrelation function of b1 and the cross-correlation function of b1 and b2. It should be noted that the autocorrelation functions have some high sidelobes near the mainlobe, and the peak level of these sidelobes is about -13.5 dB. Since this is due to the property of chirp signals, these sidelobes are ignored in the following analysis of the correlation functions.

It can be seen from Fig. 2 that there are some high sidelobes at the fixed positions of the correlation functions. These high sidelobes will cause false alarm and submerge weak targets, which has a negative influence on MIMO radar target detection. Thus, in order to improve the detection performance, we take an effort on the reason for the high

sidelobes and try to suppress the correlation interference in this letter. A theoretical analysis of the correlation function of the OFDM chirp waveforms is made in detail first. Assume $f_{\tilde{m}\tilde{n}}$ and $k_{\tilde{m}\tilde{n}}$ are the starting frequency and chirp rate of the $\tilde{n}$th subcarrier at $\tilde{m}$th subchirp duration of signal $s_q(t)$ respectively. The correlation function in (2) is further expanded as

$$\begin{aligned} & c_{pq}(\tau) \\ &= \int_{-\infty}^{+\infty} s_p(t) s_q^*(t-\tau) dt \\ &= \sum_{\tilde{m}=0}^{M-1} \sum_{\tilde{n}=0}^{N-1} \sum_{m=0}^{M-1} \sum_{n=0}^{N-1} \int_{-\infty}^{+\infty} u(t-mT_b) u(t-\tau-\tilde{m}T_b) \\ &\quad \times \exp[j2\pi (f_{mn}(t-mT_b) + k_{mn}(t-mT_b)^2/2)] \\ &\quad \times \exp[-j2\pi (f_{\tilde{m}\tilde{n}}(t-\tau-\tilde{m}T_b) \\ &\qquad + k_{\tilde{m}\tilde{n}}(t-\tau-\tilde{m}T_b)^2/2)] dt \\ &= \sum_{\tilde{m}=0}^{M-1} \sum_{\tilde{n}=0}^{N-1} \sum_{m=0}^{M-1} \sum_{n=0}^{N-1} \exp(j\varphi_{m\tilde{m}n\tilde{n}}) \int_{t_1}^{t_2} \exp[j\pi (k_{mn} - k_{\tilde{m}\tilde{n}}) t^2] \\ &\quad \times \exp\{j2\pi [k_{\tilde{m}\tilde{n}}\tau - (mk_{mn} - \tilde{m}k_{\tilde{m}\tilde{n}})T_b + f_{mn} - f_{\tilde{m}\tilde{n}}] t\} dt \end{aligned} \tag{3}$$

where

$$\begin{aligned} \varphi_{m\tilde{m}n\tilde{n}} = \pi [& -k_{\tilde{m}\tilde{n}}\tau^2 + 2(f_{\tilde{m}\tilde{n}} - k_{\tilde{m}\tilde{n}}\tilde{m}T_b)\tau \\ & + (\tilde{m} f_{\tilde{m}\tilde{n}} - m f_{mn}) 2T_b + (k_{mn}m^2 - k_{\tilde{m}\tilde{n}}\tilde{m}^2) T_b^2]. \end{aligned} \tag{4}$$

It can be seen from (3) that the correlation function between two OFDM chirp waveforms is equivalent to the sum of correlations of the subchirp signals. The autocorrelation of a subchirp signal is contained when $f_{mn} = f_{\tilde{m}\tilde{n}}$ and $k_{mn} = k_{\tilde{m}\tilde{n}}$, i.e., the same chirp signal exists in multiple subchirp durations of the correlated waveforms simultaneously. As a result, there is a high sidelobe appearing at $\tau = \pm(m - \tilde{m})T_b$ in the correlation function. Thus, the implementations of the waveforms have a crucial influence on the correlation functions. As shown in Fig. 1, the fourth subcarrier is occupied in zeroth subchirp duration and third subchirp duration of the waveform b1 simultaneously, which leads to the high sidelobe of the autocorrelation function at the delays $\pm 3T_b$ in Fig. 2(b). Hence, it is the equal chirp rates and starting frequencies that cause the repetition of the same subchirp signal and further increase the correlation interference significantly. To improve the correlation property of the waveforms, two new design schemes are proposed in the next section.

III. Proposed Waveform Diversity Design Schemes

From the analysis on correlation functions of OFDM chirp waveforms in Section II, it is known that the reason for high sidelobes is the equal chirp rates and starting frequencies. Since the chirp rates and starting frequencies are determined by the temporal durations and the modulation bandwidths of the subchirp signals, we propose to use various subchirp durations and the subcarrier bandwidths to improve the diversity of basis chirp signals. And the corresponding design methods are presented to obtain the best parameters for correlation interference suppression. Considering the complexity of hardware design and the subsequent signal processing algorithm, we propose to optimize the subcarrier bandwidths or the subchirp durations, respectively. A detailed description of the two design schemes is presented in the rest of this section.

In the first design scheme, the various subchirp durations are optimized with fixed subcarrier bandwidths, so that the waveform generation in practice becomes achievable. In order to get satisfactory correlation property, the corresponding optimization model should be established and solved for the subchirp durations. For MIMO radar waveform design, the objective function of the optimization problem should be determined beforehand. To achieve the purpose of suppressing the correlation interference, the high sidelobes should be eliminated and the correlation property should be improved. Moreover, considering specific high sidelobes may exist if the criteria of integrated sidelobes are used, the peak sidelobe level (PSL) is chosen as the objective function, which is defined as

$$\text{PSL} = \max_{\substack{p,q=1,2,\ldots,P,\, p\neq q \\ 0<\tau<T,\, -T<\upsilon<T}} \{|c_{pp}(\tau)|, |c_{pq}(\upsilon)|\} \tag{5}$$

where P denotes the number of transmit antennas. $c_{pp}(\tau)$ and $c_{pq}(\upsilon)$ represent the autocorrelation function of the pth OFDM chirp waveform and cross-correlation function between the pth waveform and qth waveform, respectively. The condition $0 < \tau < T$ is set due to the symmetry of the autocorrelation functions.

As stated above, the correlation property will be improved through optimizing the subchirp durations according to PSL in the first design scheme. Let $\boldsymbol{T}_b = [T_{b0}, T_{b1}, \ldots, T_{b(M-1)}]^T$ denote the variable consisting of M subchirp durations, then based on the objective function of PSL, the optimization model of the first design scheme is established as

$$\begin{aligned} \min_{\boldsymbol{T}_b} \quad & \max_{\substack{p,q=1,2,\ldots,P,\, p\neq q \\ 0<\tau<T,\, -T<\upsilon<T}} \{|c_{pp}(\tau)|, |c_{pq}(\upsilon)|\} \\ \text{s.t. } & 0 < T_{bm} < T, \quad m = 0, 1, \ldots, M-1 \\ & \sum_{m=0}^{M-1} T_{bm} = T \end{aligned} \tag{6}$$

where the first constraint is to restrict the range of subchirp duration values and the second constraint is to guarantee the pulse duration of the waveforms. Through solving the problem of (6), the optimal subchirp durations are found and the OFDM chirp waveforms of good correlation property are obtained subsequently.

Besides the various subchirp durations, different subcarrier bandwidths can also increase the diversity of the subchirp signals, which is the second strategy proposed for correlation interference suppression. In the second OFDM chirp waveform diversity design scheme, the various subcarrier bandwidths are optimized due to the correlation property, whereas the subchirp durations are maintained. In this case, the variable is the vector $\boldsymbol{B}_b = [B_{b0}, B_{b1}, \ldots, B_{b(M-1)}]^T$ consisting of M subcarrier bandwidths, where B_{bm} is the modulation bandwidth of the subcarriers in the mth subchirp duration. The corresponding

optimization model is represented as

$$\begin{aligned} &\min_{\boldsymbol{B}_b} \quad \max_{p,q=1,2,\ldots,P,\,p\neq q \atop 0<\tau<T,\,-T<\upsilon<T} \{|c_{pp}(\tau)|, |c_{pq}(\upsilon)|\} \\ &\text{s.t. } 0 < B_{bm} < B, \quad m = 0, 1, \ldots, M-1 \\ &\quad \sum_{m=0}^{M-1} B_{bm} = B \end{aligned} \tag{7}$$

where the first constraint is to limit the values of modulation bandwidths and the second constraint is to ensure the available bandwidth of the waveform. It is noted that before calculating the frequency distribution to obtain the waveforms, the occupied subcarriers should be rearranged as some groups of complete frequency codes.

Both of the optimization models in (6) and (7) are constrained nonlinear problems and sequential quadratic programming (SQP) [15] is usually used as the solver. Hence, we also apply SQP to the optimization in this letter. It should be mentioned that the initial elements of the variables are chosen as random values in the absence of prior information. Through solving the optimization problems above, the subchirp durations or subcarrier bandwidths of the OFDM chirp diverse waveform are obtained, and the signals are designed accordingly.

IV. Design Examples and Simulation Results

In this section, we give some design examples and simulation results to verify the effectiveness of the proposed OFDM chirp diverse waveform design methods. As described above, the waveforms with various subchirp durations or subcarrier bandwidths will be designed, respectively. The performance of the waveforms will be evaluated by the correlation function, which is an effective tool related to target detection performance.

The parameters of the OFDM chirp diverse waveform are assumed as follows. The available bandwidth is $B = 400$ MHz, the pulse duration is $T = 8$ μs, the number of subchirp durations is $M = 8$, and the number of subcarriers is $N = 8$. Based on the obtained frequency codes of the conventional waveforms in Fig. 1, our proposed methods are performed for correlation interference suppression. For simplicity, we just show the results related to waveforms b1 and b2.

Fig. 3(a) illustrates the implementations of our designed waveforms with various subchirp durations, whereas Fig. 3(b) shows that with diverse subcarrier bandwidths. In Fig. 3(b), the rearranged two frequency coding sequences of occupied subcarriers in waveforms b1 and b2 are {5, 4, 7, 1, 3, 2, 8, 6; 7, 1, 3, 5, 8, 6, 4, 2} and {1, 3, 5, 8, 2, 4, 6, 7; 8, 6, 1, 3, 5, 7, 2, −4}, respectively. To distinguish them, the solid line and dashed-dotted line are used for the first and second coding sequences, respectively, in Fig. 3(b). The grids of subcarrier bandwidths in Fig. 3 are plotted based on the first complete frequency coding sequence of the waveform. For the sake of clarity, the obtained waveform parameters $\boldsymbol{T}_b$ and $\boldsymbol{B}_b$ are given in Table I. The f_{mn}s of designed OFDM signals with various subchirp durations can be obtained easily through Fig. 3(a), whereas those with diverse subcarrier bandwidths in Fig. 3(b) are necessary to be shown in Table I.

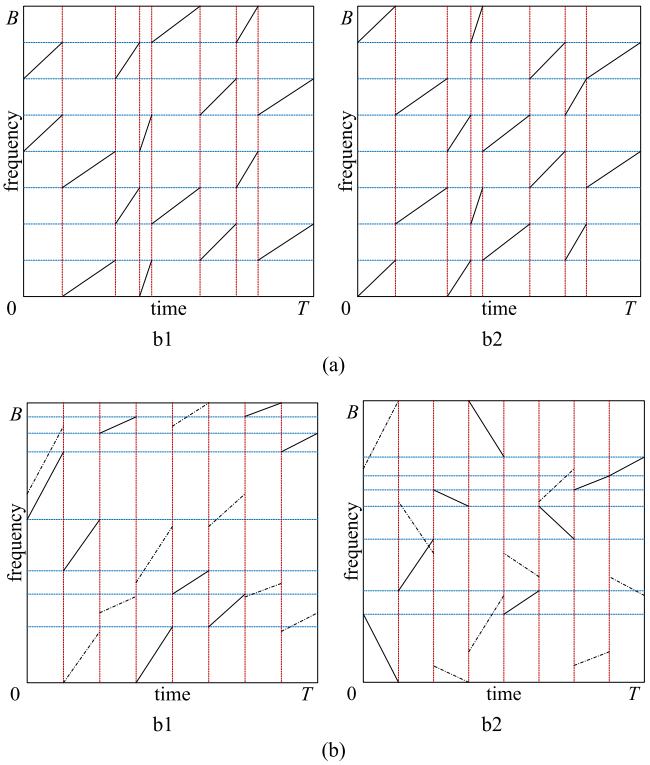

Fig. 3. Implementations of our designed OFDM chirp waveforms. (a) Designed waveforms with various subchirp durations. (b) Designed waveforms with various subcarrier bandwidths.

TABLE I

Parameters of the Designed Waveforms in Fig. 3

mth subchirp duration		0	1	2	3	4	5	6	7
T_{bm} in Fig.3(a)/μs		1.1	1.5	0.7	0.1	1.4	1	0.6	1.6
B_{bm} in Fig.3(b)/MHz		90	75	25	80	35	45	20	30
f_{mn} of b1 in Fig.3(b)/MHz	1*st*	235	160	355	0	125	80	380	325
	2*nd*	275	0	105	150	365	230	130	75
f_{mn} of b2 in Fig.3(b)/MHz	1*st*	90	125	270	400	90	245	270	290
	2*nd*	310	265	25	45	190	265	25	155

It can be seen from Fig. 3(a) that our designed OFDM chirp waveforms have different temporal durations, which result in unequal chirp rates of the basis chirp signals. And the subchirp signals of the waveforms in Fig. 3(b) have diverse modulation bandwidths, which lead to unequal chirp rates and various starting frequencies. On the other hand, the basis signals of the conventional OFDM chirp waveforms in Fig. 1 have equal or reverse chirp rates and fixed starting frequencies. Since the reason for high sidelobes of the correlation functions is the equal variables, the high correlation sidelobes are suppressed due to the various parameters of subchirps in the designed waveforms. To validate the effectiveness of the proposed methods, we calculate the correlation property of the designed waveforms. Fig. 4 plots the autocorrelation functions and cross-correlation functions of the waveforms in Fig. 3.

Comparing the result in Fig. 4 with that in Fig. 2(b), it shows that the correlation functions of the conventional waveforms and our designed waveforms are different. It can be seen from Fig. 2 that the correlation functions of the conventional waveforms have some high grating sidelobes, which are naturally judged as small targets and easily cause

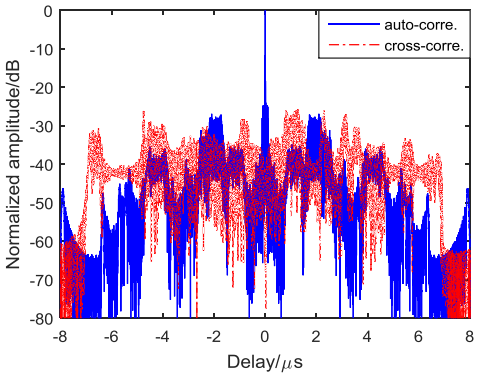

(a)

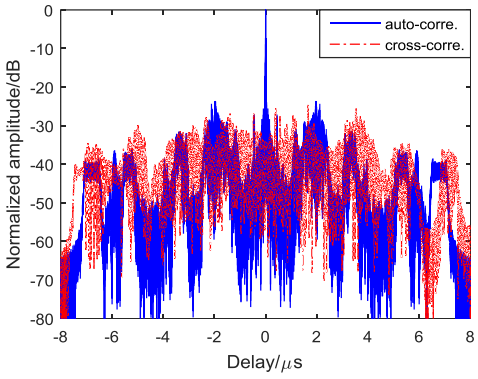

(b)

Fig. 4. Correlation functions of our designed OFDM chirp waveforms. (a) Correlation functions of the designed waveforms in Fig. 3(a). (b) Correlation functions of the designed waveforms in Fig. 3(b).

TABLE II
COMPARISON BETWEEN CONVENTIONAL WAVEFORMS AND DESIGNED WAVEFORMS

	Waveforms	Conventional	Proposed method 1	Proposed method 2
APSL /dB	a1 and a1	-34.23	-37.35	-35.34
	b1 and b1	-8.52	-26.97	-25.22
CPL /dB	a1 and a2	-18.06	-28.20	-26.36
	b1 and b2	-10.59	-25.73	-24.64

false detection. The reason is the same chirp signal exists in some subchirp durations simultaneously. Since the subchirp durations or subcarrier bandwidths are various and optimized in the proposed methods, it is shown from Fig. 4(a) and (b) that the designed waveforms do not have obvious high sidelobes, and the sidelobe levels are more stable than that of the conventional waveforms. Hence, the suppression of correlation interference is successfully achieved and the designed waveforms have considerable correlation properties. The effectiveness of the proposed design schemes is verified and the detection performance of MIMO radar is improved.

In order to explore the performance of the proposed methods in depth, Table II lists the autocorrelation PSLs (APSLs) and cross-correlation peak levels (CPLs) of the conventional waveforms and our designed waveforms.

From Table II, it is observed that our designed OFDM chirp waveforms have lower APSLs and CPLs than those of the conventional waveforms. The conventional waveforms have high correlation sidelobes due to the equal subchirp durations and the same subcarrier bandwidth, whereas the correlation properties are improved by optimizing the various parameters in the proposed methods. The results in Table II also show that the two proposed design schemes have comparable performance in OFDM chirp diverse waveform design. The lack of our proposed methods is the large computation complexity for solving the constrained nonlinear problems, which is planned to be studied in our future work.

V. CONCLUSION

The OFDM chirp diverse waveform becomes widely applied in MIMO radar since its superiorities in practical applications. However, there are some high sidelobes existing in its correlation functions, which has a serious influence in target detection. In order to eliminate the high sidelobes to improve target detection performance, the reason for high sidelobes is analyzed and two new OFDM chirp waveform diversity design schemes are proposed. The various subchirp durations or different subcarrier bandwidths are optimized for PSL reduction. The numerical examples show that the designed waveforms have better correlation performance than the conventional waveforms.

REFERENCES

[1] E. Fishler, A. Haimovich, R. Blum, D. Chizhik, L. Cimini, and R. Valenzuela, "MIMO radar: An idea whose time has come," in *Proc. IEEE Radar Conf.*, Philadelphia, PA, USA, Apr. 2004, pp. 71–78.
[2] E. Fishler, A. Haimovich, R. Blum, L. Cimini, D. Chizhik, and R. Valenzuela, "Performance of MIMO radar systems: Advantages of angular diversity," in *Proc. 38th Asilomar Conf. Signals, Syst., Comput.*, vol. 1. Nov. 2004, pp. 305–309.
[3] L. Xu, J. Li, and P. Stoica, "Target detection and parameter estimation for MIMO radar systems," *IEEE Trans. Aerosp. Electron. Syst.*, vol. 44, no. 3, pp. 927–939, Jul. 2008.
[4] H. Deng, "Polyphase code design for Orthogonal Netted Radar systems," *IEEE Trans. Signal Process.*, vol. 52, no. 11, pp. 3126–3135, Nov. 2004.
[5] P. Stoica, H. He, and J. Li, "New algorithms for designing unimodular sequences with good correlation properties," *IEEE Trans. Signal Process.*, vol. 57, no. 4, pp. 1415–1425, Apr. 2009.
[6] N. Levanon, "Multifrequency complementary phase-coded radar signal," in *IEE Proc.-Radar, Sonar Navigat.*, vol. 147, no. 6, pp. 276–284, Dec. 2000
[7] W.-Q. Wang, "Mitigating range ambiguities in high-PRF SAR with OFDM waveform diversity," *IEEE Geosci. Remote Sens. Lett.*, vol. 10, no. 1, pp. 101–105, Jan. 2013.
[8] S. Sen, G. Tang, and A. Nehorai, "Multiobjective optimization of OFDM radar waveform for target detection," *IEEE Trans. Signal Process.*, vol. 59, no. 2, pp. 639–652, Feb. 2011.
[9] M. A. Sebt, A. Sheikhi, and M. M. Nayebi, "Orthogonal frequency-division multiplexing radar signal design with optimised ambiguity function and low peak-to-average power ratio," *IET Radar, Sonar Navigat.*, vol. 3, no. 2, pp. 122–132, Apr. 2009.
[10] T. Huang and T. Zhao, "Low PMEPR OFDM radar waveform design using the iterative least squares algorithm," *IEEE Signal Process. Lett.*, vol. 22, no. 11, pp. 1975–1979, Nov. 2015.
[11] J.-H. Kim, M. Younis, A. Moreira, and W. Wiesbeck, "A novel OFDM chirp waveform scheme for use of multiple transmitters in SAR," *IEEE Geosci. Remote Sens. Lett.*, vol. 10, no. 3, pp. 568–572, May 2013.
[12] J. H. Kim, M. Younis, A. Moreira, and W. Wiesbeck, "Spaceborne MIMO synthetic aperture radar for multimodal operation," *IEEE Trans. Geosci. Remote Sens.*, vol. 53, no. 5, pp. 2453–2466, May 2015.
[13] J. Wang, L.-Y. Chen, X.-D. Liang, C.-B. Ding, and K. Li, "Implementation of the OFDM chirp waveform on MIMO SAR systems," *IEEE Trans. Geosci. Remote Sens.*, vol. 53, no. 9, pp. 5218–5228, Sep. 2015.
[14] W.-Q. Wang, "MIMO SAR OFDM chirp waveform diversity design with random matrix modulation," *IEEE Trans. Geosci. Remote Sens.*, vol. 53, no. 3, pp. 1615–1625, Mar. 2015.
[15] N. Rau, *Optimization Principles: Practical Applications to the Operation and Markets of the Electric Power Industry*. Hoboken, NJ, USA: Wiley, 2003, pp. 177–243.